Journal of Orthopaedic Translation 23 (2020) 77–88

Contents lists available at ScienceDirect

Journal of Orthopaedic Translation

journal homepage: www.journals.elsevier.com/journal-of-orthopaedic-translation

Original Article

Preclinical safety and efficacy of 24R,25-dihydroxyvitamin D_3 or lactosylceramide treatment to enhance fracture repair

Corine Martineau [a], Martin Kaufmann [b,c], Alice Arabian [a], Glenville Jones [b], René St-Arnaud [a,d,e,f,g,*]

[a] Research Centre, Shriners Hospitals for Children – Canada, Montreal, Quebec, H4A 0A9, Canada
[b] Department of Biomedical and Molecular Sciences, Queen's University, Kingston, Ontario, K7L 3N6, Canada
[c] Department of Surgery, Queen's University, Kingston, Ontario, K7L 3N6, Canada
[d] Department of Human Genetics, McGill University, Montreal, Quebec, H3A 1A1, Canada
[e] Department of Surgery, McGill University, Montreal, Quebec, H3A 1A1, Canada
[f] Department of Medicine, McGill University, Montreal, Quebec, H3A 1A1, Canada
[g] Research Institute of the McGill University Health Centre, Montreal, Quebec, H3H 2R9, Canada

ARTICLE INFO

Keywords:
24,25-dihydroxyvitamin D
Bone
Family with sequence similarity 57B, isoform 2 (FAM57B2)
Fracture
Lactosylceramide
Repair
Tram-Lag1-CLN8 domain containing 3B isoform 2 (TLCD3B2)

ABSTRACT

Background/Objective: *Cyp24a1*-null mice deficient in $24,25(OH)_2D_3$ display impaired callus formation during the endochondral phase of bone fracture repair. The $24,25(OH)_2D_3$ metabolite acted by binding to the TLC domain containing 3B isoform 2 (TLCD3B2, previously named FAM57B2) effector protein, which then synthesizes lactosylceramide (LacCer). Treatment with $24,25(OH)_2D_3$ or LacCer restored callus size and mechanical properties in *Cyp24a1*-null mice.

Methods: To assess the safety of these molecules and test their efficacy for bone healing in wild-type, non-genetically modified mice, we treated 12-week-old, osteotomized C57BL/6 female mice with each compound for up to 21 days post-osteotomy. Control cohorts were injected with vehicle.

Results: Neither compound was found to exhibit any nephro- nor hepato-toxicity. Calcemia remained stable throughout the experiment and was unaffected by either treatment. Supplementation with $24,25(OH)_2D_3$ increased circulating levels of this metabolite about 8-fold, decreased $1,25(OH)_2D_3$ levels, and significantly increased circulating $1,24,25(OH)_3D_3$ levels, suggesting 1?-hydroxylation of $24,25(OH)_2D_3$. TLCD3B2 was found to be expressed in fracture callus at the surface of unmineralized or pre-mineralized cartilage on day 10 and day 12 post-osteotomy and to progressively recede to become undetectable by day 18. Treatment with $24,25(OH)_2D_3$ or LacCer reduced the number of TLCD3B2-positive cells. Both treatments also significantly increased stiffness and elastic modulus of the healing bone callus.

Conclusion: Exogenous administration of $24,25(OH)_2D_3$ or LacCer improved the biomechanical properties of repaired bones in wild-type animals without affecting circulating calcium levels or other blood parameters, demonstrating preclinical safety and efficacy.

Translational potential: Our data suggest the use of 24R,25-dihydroxyvitamin D_3 or lactosylceramide for ameliorating fracture healing in clinical practice.

Introduction

An estimated 6 million bone fractures occur yearly in North America, with a risk factor ranging between 150 and 250 per 100,000 [1]. Fracture risk augments with age in the general population and correlates with bone mineral density (BMD) and osteopenia incidence [2]. Moreover, developmental skeletal disorders such as osteogenesis imperfecta can dramatically increase these odds [3]. Bone disorders, whether metabolic or developmental, significantly increase the rate of complication such as delayed union, malunion, nonunion or refracture [2,4]. There thus exists an unmet clinical need to ameliorate fracture management strategies, especially for at-risk populations.

Bone fracture healing involves a series of tightly regulated events [5]. It begins with the formation of a haematoma at the fracture site towards

* Corresponding author. Research Centre, Shriners Hospitals for Children – Canada, 1003 Decarie Boulevard, Montreal, Quebec, H4A 0A9, Canada.
E-mail address: rst-arnaud@shriners.mcgill.ca (R. St-Arnaud).

https://doi.org/10.1016/j.jot.2020.03.013
Received 10 July 2019; Received in revised form 5 February 2020; Accepted 25 March 2020
Available online 27 April 2020

which immune and precursor cells migrate, proliferate and differentiate. The formation of a fibrocartilaginous callus then follows, stabilizing the fracture and progressively mineralizing through endochondral and intramembranous ossification. The mineralized callus is subsequently remodelled into true lamellar bone, thus restoring structure and function to the affected limb. Alterations in this process extend hospitalization time, augment risk of complication and significantly impair quality of life in affected patients [6]. Numerous risk factors ranging from genetics, pharmaceutical treatments and lifestyle have all been shown to impact fracture repair outcome [7].

Although it is generally accepted that vitamin D deficiency at the time of fracture increases the risk of complication [8], the beneficial effects of vitamin D supplementation during fracture repair remain debated [9]. Several confounding factors exist, namely the high number of vitamin D metabolites, coadministration of calcium supplements, vitamin D status and age of the tested cohorts, as well as lack of focus on time points. Over two decades ago, the 24R,25-dihydroxyvitamin D_3 [24,25$(OH)_2D_3$] metabolite has been suggested to participate in the fracture repair process in chicks [10]. However, this correlation remains equivocal in human beings as 24,25$(OH)_2D_3$ levels remain stable throughout the healing process, at least in older patients [11].

Recently, our team has shown that *Cyp24a1*-null mice, unable to produce 24,25$(OH)_2D_3$, display impaired callus formation during the endochondral phase of fracture repair [12]. The 24,25$(OH)_2D_3$ metabolite acted by binding to the Tram-Lag1-CLN8 (TLC) domain containing 3B isoform 2 (TLCD3B2, new Human Genome Organization Gene Nomenclature Committee name and symbol for FAM57B2) and inducing synthesis of lactosylceramide (LacCer) by TLCD3B2. Cartilage-specific deletion of *Tlcd3b* phenocopied the impaired fracture repair observed in *Cyp24a1*-null mice, and the physiological relevance of the signalling cascade was further highlighted by rescue experiments. Subcutaneous administration of 24,25$(OH)_2D_3$ or LacCer restored both callus size and mechanical properties in *Cyp24a1*-null mice, whereas cartilage-specific deletion of *Tlcd3b* could only be rescued with exogenous LacCer supplementation [12]. In this follow-up study, we aimed at testing the safety and efficacy of these two compounds in ameliorating fracture healing of nongenetically modified mice, and to identify a time range for efficient intervention.

Materials and methods

Animals

Ten-week-old female mice from the C57BL/6 strain were ordered from Charles River (Senneville, QC, Canada) and left in quarantine to acclimate until 12 weeks of age. All animals were housed five per cages at 25 °C with a 12 h dark/12 h light cycle and *ad libitum* access to food and water.

All standard operating procedures were approved by the IACUC of Shriners Hospitals for Children – Canada (AUP 4138), as part of the McGill University animal ethics and care program, and followed the guidelines of the Canadian Council on Animal Care.

Intramedullary rodded tibial osteotomy

The surgical procedure was performed as described in Martineau et al. [12]. Briefly, mice under general isoflurane anaesthesia had an incision made above the right knee to free the patellar ligament from lateral tissue. A 26G needle was gently pushed through the tibial plateau allowing insertion of a 25G spinal needle wire guide under the patellar ligament down the medullary canal. The needle was pulled out, the wire guide was bent 90°, cut at the tibial plateau and secured by a mattress suture on either side of the patellar ligament. The tibial shaft was exposed and cut using micro scissors about 2–3 mm above the tibiofibular junction. Topical analgesics were applied at the wound site, then the skin was sutured. Carprofen was provided at the time of surgery and for the following 48 h postosteotomy. After isoflurane general anaesthesia and exsanguination through cardiac puncture, mice were euthanized by cervical dislocation on Days 10, 12, 15, 18 and 21. Serum and bones were harvested for analysis for each time point.

LacCer and 24,25$(OH)_2D_3$ treatment

Seventy-two hours postosteotomy, mice were injected subcutaneously daily with either 24,25$(OH)_2D_3$ (6.7 μg/kg daily in 50 μL propylene glycol with trace ethanol for vitamin D metabolite solubility); C18-LacCer (50 μg/kg daily in 50 μL propylene glycol with trace dimethyl sulfoxide (DMSO) for solubility) or the propylene glycol with trace ethanol or DMSO vehicle until sacrifice, as described previously [12].

Serum biochemistry

After harvest of whole blood through cardiac puncture, serum was isolated by centrifugation (20 min at 2000*g*, 4 °C), aliquoted and frozen at −80 °C until analysis. Serum biochemistry for liver and kidney function (aspartate transaminase [AST], alanine transaminase [ALT], gamma glutamyltransferase [GGT], total bilirubin, glucose, albumin, total protein, creatine kinase [CK], blood urea nitrogen and creatinine) was outsourced to the McGill Comparative Medicine Animal Resources Centre; samples were streamlined through the Vitros 250 Chemistry System (Ortho Clinical Diagnostics, Markham, ON, Canada). Alkaline phosphatase (ALP) was measured using the QuantiChrom Alkaline Phosphatase Assay Kit (BioAssay Systems, Hayward, CA, USA); calcium and phosphorus were measured with the SEKURE chemistry calcium and phosphorus kits (Sekisui Diagnostics, Kent, United Kingdom) and cFGF-23 was measured with the ELISA Mouse/Rat cleaved FGF-23 Kit (Quidel Corporation, Athens, OH, USA). Bone formation and resorption markers, osteocalcin (OCN; Immunotopics, San Clemente, CA, USA) and carboxy-terminal collagen crosslinks (CTX; Immunodiagnostic Systems, East Boldon, United Kingdom) were measured using ELISA kits.

Vitamin D metabolites were assayed by liquid chromatography–tandem mass spectrometry (LC-MS/MS) following 4-[2-(3,4-Dihydro-6,7-dimethoxy-4-methyl-3-oxo-2-quinoxalinyl)ethyl]-3H-1,2,4-triazole-3,5(4H)-dione (DMEQ-TAD) derivatization as described previously [13]. For analysis of 25$(OH)D_3$, 24,25$(OH)_2D_3$ and 25$(OH)D_3$-26, 23-lactone, 25 μL volumes of mouse serum and calibrators were spiked with internal standards and diluted to 300 μL with water. Proteins were precipitated by sequentially adding 100 μL of 0.1 M HCl, 150 μL 0.2 M zinc sulphate, and 450 μL methanol, with vortexing after the addition of each component. Tubes were centrifuged and supernatants were extracted with 700 μL of methyl tertiary butyl ether and 700 μL hexane, and vortexed. For analysis of 1,25$(OH)_2D_3$ and 1,24,25$(OH)_3D_3$, 125 μL volumes of mouse serum and calibrators were spiked with internal standards, and extracted with 100 μL of anti-1,25$(OH)_2D_3$ antibody slurry (Immundiagnostik AG, Bensheim, Germany) for 2 h at room temperature by end-over-end rotation. Using centrifugation, the slurry was isolated and rinsed four times with 400 μL of water, and vitamin D metabolites were eluted with 400 μL of ethanol. Dried residues from both extraction platforms were derivatized by addition of 0.1 mg/mL DMEQ-TAD dissolved in ethyl acetate for 30 min at room temperature in the dark and then a second time for 60 min. The reaction was stopped by addition of ethanol, and the samples were dried and redissolved in a 60:40 methanol/water running buffer. LC-MS/MS analysis was performed using an Acquity UPLC connected in-line with a Xevo TQ-S mass spectrometer in electrospray-positive mode (Waters Corporation, Milford, MA, USA). Chromatographic separations were achieved using a BEH-phenyl ultra-performance LC (UPLC) column (1.7 μm, 2.1 × 50 mm) (Waters) for 25$(OH)D_3$ analysis, or a Cortecs C18$^+$ UPLC column (2.7 μm,

2.1 × 100 mm) (Waters) for 1,25$(OH)_2D_3$ analysis, using a methanol–water–based gradient solvent system as previously described [13].

Microcomputed tomography

Calluses and contralateral tibiae destined to microcomputed tomography (microCT) analysis were harvested in phosphate-buffered saline (PBS), scanned with a model 1272 SkyScan microCT system (Bruker SkyScan, Kontich, Belgium) at 65 kV, 142 μAmp, 5 μm resolution and a 0.5° rotation using a 0.5-mm aluminium filter, and frozen at −20 °C until three-point bending tests (3PBTs). Raw data sets were reconstructed with InstaRecon software (Bruker SkyScan) and analyzed with CTAn software (Bruker SkyScan). Volumes of interest consisted of 400 slices (2 mm thick) above and below the osteotomy site, for a total volume of 4 mm^3, and used to obtain the average callus area values used to normalize the 3PBTs. Volumetric BMD (vBMD) was evaluated in callus tissue by comparing to hydroxyapatite standard rods (Bruker SkyScan).

3PBTs

For the 3PBTs, contralateral and callus tibiae were thawed overnight at room temperature and tested for mechanical properties using an Instron model 5943 single-column table frame machine (Instron, Norwood, MA, USA). A load-sensing cell was applied on the widest part of the callus, or 2–3 mm above the tibiofibular junction in the case of intact tibiae, which were held by holders set 6 mm apart. The raw output used for comparison was stiffness (N/mm), maximum load (N) and load at yield (N), which were further normalized to elastic modulus (MPa), ultimate strength (MPa) and strength at yield (MPa) using the callus area of the widest part of the callus as evaluated through microCT.

Histology

Bones destined to histology and immunohistochemistry were harvested in 70% ethanol–1% glycerol and stored at −20 °C until processing. Bones were sequentially dehydrated at 4 °C and infiltrated with low-temperature polymerizing methylmethacrylate (MMA) solutions I, II and III containing, respectively, 0%, 4% and 8% benzoyl peroxide as described by Erben [14]. Bones were embedded in MMA solution III supplemented with 0.4% 4-N,N,N,N-trimethylaniline (MilliporeSigma, Oakville, ON, Canada) and left to polymerize at −20 °C for 3 days under N_2(g) atmosphere. Blocks were sectioned at 5 μm thickness using a rotary microtome equipped with a tungsten blade (Leica Microsystems, Concord, ON, Canada), stretched onto poly-L-lysine–coated superfrost slides, stacked with plastic clamps, and left to dry overnight at room temperature. For staining, sections were deplastified in xylene (1 h), ethylene glycol monoethyl ether acetate (1 h), then rehydrated from ethanol to water and stained with Alcian blue H&E Y-orange G trichrome. Images were taken using a Leica DMR microscope (Leica Microsystems) connected to a digital DP70 camera (Olympus Corporation, Tokyo, Japan). Image area measurements of Alcian blue H&E Y-orange G trichrome-stained sections were performed using ImageJ as described in the figure legend.

Immunohistochemistry

Sections were deplastified and rehydrated as stated above, then blocked and permeabilized overnight at 4 °C in PBS containing 10% fetal bovine serum (Invitrogen, Thermo Fisher Scientific, Saint-Laurent, QC, Canada) and 0.1% Triton-X100 (Sigma-Aldrich, Oakville, ON, Canada). After rinsing for 3 × 10 min in PBS, the sections were incubated for 1 h at room temperature with the rabbit anti-TLCD3B polyclonal antibody from Biorbyt (#orb183613, San Francisco, CA, USA) diluted 1:150 in PBS containing 10% normal rabbit serum (Invitrogen) and 0.1% Triton-X100. Sections were rinsed 3 × 10 min in PBS, then incubated 1 h at room temperature with goat anti-rabbit secondary IgG coupled to Alexa 594 (Invitrogen) diluted 1:1000 in PBS containing 10% normal goat serum and 0.1% Triton-X100. Sections were rinsed 3 × 10 min in PBS, mounted with ProLong Gold with DAPI (Invitrogen) then dried overnight at room temperature. Images were taken using a Leica DMR microscope (Leica Microsystems) connected to a digital PhotoFluor LM75 fluorescent camera (89 North, Williston, VT, USA). Cell counting of TLCD3B-immunostained sections was performed with ImageJ as mentioned in the figure legend.

Statistics

All graphs and analyses were performed with the Prism 5 software (GraphPad, La Jolla, CA, USA). When applicable, normality of data distribution was assessed using the D'Agostino-Pearson test. Student's *t* tests were applied when comparing two groups, or a two-way analysis of variance was applied when comparing three or more groups together, followed by either a Dunnett's post-test (when comparing all groups to a single control group) or a Bonferroni's post-test (when comparing all groups among each other). Strength of association was evaluated using the Spearman rank-order coefficient (r_S). Statistical significance was set at a p value of 0.05 or below.

Results

We recently reported that 24,25$(OH)_2D_3$ or LacCer treatment restores callus size and mechanical properties of healing bones in *Cyp24a1*-null mice [12]. To assess the safety of these molecules, test the efficacy of the compounds for bone healing in nongenetically modified mice and narrow down the time range at which the TLCD3B2 protein acts during fracture repair, we treated 12-week-old, osteotomized C57Bl6 female mice with each compound for up to 21 days postosteotomy. Control cohorts were injected with the corresponding vehicle.

Kidney and liver function

A blood biochemistry panel was performed at each time point for either treatment to observe liver and kidney function. For treatment with either 24,25$(OH)_2D_3$ (Table 1) or LacCer (Table 2), total protein, albumin-to-globulin ratio, blood urea nitrogen, total bilirubin, ALT, AST, GGT and CK were all within normal ranges. Inexplicably, the 24,25$(OH)_2D_3$ treatment significantly reduced CK levels on Day 18 postosteotomy, but concentrations returned to vehicle values on Day 21.

Serum albumin and creatinine were found to be below reference values in all mice at every time point. However, glucose remained slightly above normal ranges, presumably due to increased metabolic demand during fracture repair [15]. Overall, no parameter reached a critical value at any time point for either treatment.

Mineral homeostasis and bone turnover

Total ALP showed an increasing trend on Days 18 and 21 post-osteotomy for both 24,25$(OH)_2D_3$ (Fig. 1A) and LacCer (Fig. 1E) supplementation, and this increase was statistically significant for the 24,25$(OH)_2D_3$ treatment on Day 18 compared to vehicle-treated mice. Serum calcium levels remained stable at the upper limit of the normal range throughout the experiment and were unaffected by either treatment (Fig. 1B and F). On the other hand, phosphorus levels (Fig. 1C and G) varied somewhat during fracture repair, sometimes exceeding the upper normal limit by a small margin, presumably linked to metabolic demand for mineralization [16]. The 24,25$(OH)_2D_3$ treatment significantly influenced serum phosphorus levels on Days 18 and 21 post-osteotomy, but LacCer had no significant impact. Circulating OCN levels, an index of bone formation, showed a similar trend as phosphorus in Day 18 samples from the 24,25$(OH)_2D_3$-treated group (Table 1). Serum levels of the bone resorption marker CTX were not significantly affected by either treatment (Tables 1 and 2).

Table 1
Blood biochemistry values in 12-week-old vehicle- or 24,25D_3-treated female C57BL/6 mice 10–21 days postosteotomy.

Treatment	Vehicle					$24,25(OH)_2D_3$				
Day	10	12	15	18	21	10	12	15	18	21
Total protein (33–66 g/L)	39.7 ± 0.4	40.5 ± 0.6	42.8 ± 1.1	41.5 ± 0.3	43.2 ± 0.5	40.3 ± 0.4	40.8 ± 0.7	42.7 ± 1.1	43.2 ± 1.3	41.0 ± 0.4
Albumin (25–48 g/L)	20.2 ± 0.5	20.3 ± 0.5	22.2 ± 0.7	21.5 ± 0.2	21.7 ± 0.7	20.8 ± 0.2	20.5 ± 0.7	22.2 ± 0.7	22.5 ± 0.9	21.0 ± 0.3
AGR (0.8–1.4)	1.05 ± 0.04	1.02 ± 0.03	1.08 ± 0.03	1.08 ± 0.03	1.02 ± 0.06	1.08 ± 0.02	1.05 ± 0.04	1.10 ± 0.06	1.05 ± 0.02	1.07 ± 0.04
Glucose (5–10.7 mmol/L)	15.2 ± 1.0	15.4 ± 0.7	16.4 ± 0.6	17.7 ± 0.5	15.1 ± 0.7	16.5 ± 0.5	16.2 ± 1.2	14.4 ± 0.6	14.0 ± 1.3	15.3 ± 0.5
BUN (6.4–10.4 mmol/L)	7.10 ± 0.36	7.40 ± 0.30	8.30 ± 0.47	7.58 ± 0.16	7.93 ± 0.45	7.45 ± 0.26	7.57 ± 0.36	8.23 ± 0.38	6.07 ± 0.45	7.95 ± 0.25
Creatinine (18–71 pmol/L)	13.0 ± 0.0	13.0 ± 0.0	13.0 ± 0.0	13.0 ± 0.0	13.0 ± 0.0	13.0 ± 0.0	14.2 ± 1.0	13.0 ± 0.0	13.0 ± 0.0	13.0 ± 0.0
Tot. bil. (2–15 pmol/L)	3.00 ± 0.26	2.83 ± 0.17	3.28 ± 0.52	3.83 ± 0.31	3.83 ± 0.31	3.67 ± 0.49	3.50 ± 0.22	4.45 ± 1.20	6.33 ± 2.74	3.50 ± 0.22
ALT (28–132 U/L)	42.7 ± 0.9	41.0 ± 1.1	46.2 ± 1.2	49.8 ± 8.2	43.5 ± 1.5	53.8 ± 9.4	41.8 ± 4.1	43.5 ± 1.2	39.7 ± 1.2	42.5 ± 0.4
AST (59–247 U/L)	73.8 ± 2.4	81.8 ± 6.2	80.5 ± 4.0	84.7 ± 11.3	85.3 ± 9.2	97.0 ± 13.5	87.5 ± 8.6	87.0 ± 4.7	78.2 ± 4.8	80.8 ± 4.6
GGT (0 U/L)	10 ± 0	10 ± 0	10 ± 0	10 ± 0	10 ± 0	10 ± 0	10 ± 0	10 ± 0	10.5 ± 0.5	10 ± 0
CK (68–1070 U/L)	654.8 ± 157.3	1088.0 ± 132.2	913.0 ± 41.8	847.5 ± 146.3	313.3 ± 92.9	677.5 ± 76.8	916.3 ± 78.0	1064.2 ± 190.7	**254.5 ± 66.8**[a]	385.2 ± 49.9
OCN (ng/mL)	102.7 ± 11.9	NA	156.4 ± 24.4	184.0 ± 12.0	108.5 ± 15.9	126.3 ± 6.6	NA	173.3 ± 18.0	**109.4 ± 20.4**[a]	155.8 ± 16.1
CTX (ng/mL)	18.5 ± 1.8	NA	17.8 ± 0.8	23.1 ± 1.7	17.2 ± 1.7	17.4 ± 1.2	NA	18.1 ± 1.3	23.3 ± 2.6	18.8 ± 0.9

Parameters are followed by mice normal range values and/or units in parentheses. Data are mean ± SEM, $n = 6$ mice/group except for OCN and CTX where $n = 5$ mice/group. Bold signifies statistically significant change vs. vehicle.

AGR = albumin-to-globulin ratio; ALT = alanine transaminase; ANOVA = analysis of variance; AST = aspartate transaminase; BUN = blood urea nitrogen; CK = creatine kinase; CTX = carboxy-terminal collagen crosslinks; GGT = gamma-glutamyl transferase; NA = not available; OCN = osteocalcin; SEM = standard error of the mean; Tot. bil. = total bilirubin.

[a] $p < 0.01$ versus vehicle of corresponding time point, two-way ANOVA followed by Bonferroni post-test.

Table 2
Blood biochemistry values in 12-week-old vehicle- or LacCer-treated female C57BL/6 mice 10–21 days postosteotomy.

Treatment	Vehicle					LacCer				
Day	10	12	15	18	21	10	12	15	18	21
Total protein (33–66 g/L)	41.5 ± 1.2	42.8 ± 1.1	42.0 ± 0.4	42.0 ± 0.6	42.5 ± 1.0	40.7 ± 0.3	41.8 ± 0.6	40.2 ± 0.4	42.2 ± 0.8	42.8 ± 0.5
Albumin (25–48 g/L)	21.5 ± 0.8	22.3 ± 0.8	21.8 ± 0.4	21.7 ± 0.2	22.7 ± 0.6	21.2 ± 0.7	21.7 ± 0.3	20.7 ± 0.3	22.2 ± 0.4	22.8 ± 0.3
AGR (0.8–1.4)	1.07 ± 0.02	1.05 ± 0.03	1.08 ± 0.03	1.07 ± 0.02	1.12 ± 0.03	1.10 ± 0.06	1.08 ± 0.02	1.10 ± 0.03	1.10 ± 0.00	1.15 ± 0.02
Glucose (5–10.7 mmol/L)	11.4 ± 1.1	13.1 ± 1.1	13.6 ± 0.5	13.6 ± 0.5	10.6 ± 0.8	13.5 ± 0.5	13.6 ± 0.5	11.7 ± 0.6	11.1 ± 1.4	13.5 ± 1.3
BUN (6.4–10.4 mmol/L)	7.08 ± 0.50	6.55 ± 0.22	7.1 5 ± 0.43	7.42 ± 0.40	6.97 ± 0.38	7.57 ± 0.29	6.27 ± 0.30	7.25 ± 0.22	8.90 ± 0.21	6.80 ± 0.22
Creatinine (18–71 pmol/L)	13 ± 0	13 ± 0	13 ± 0	13 ± 0	13 ± 0	13 ± 0	13 ± 0	13 ± 0	13 ± 0	13 ± 0
Tot. bil. (2–15 pmol/L)	3.17 ± 0.31	5.17 ± 1.80	3.62 ± 0.46	3.33 ± 0.21	2.67 ± 0.33	3.17 ± 0.31	3.50 ± 0.34	2.83 ± 0.31	3.17 ± 0.31	3.83 ± 0.48
ALT (28–132 U/L)	46.2 ± 1.7	44.3 ± 1.8	40.3 ± 1.1	44.3 ± 1.0	46.7 ± 0.7	44.5 ± 0.8	39.0 ± 0.9	44.5 ± 1.9	43.8 ± 1.0	43.8 ± 2.0
AST (59–247 U/L)	77.0 ± 4.1	84.5 ± 5.9	71.3 ± 2.0	79.5 ± 3.9	105.5 ± 14.5	76.8 ± 5.2	84.2 ± 9.2	81.8 ± 8.4	77.3 ± 6.8	71.7 ± 6.4
GGT (0 U/L)	10 ± 0	10 ± 0	10 ± 0	10 ± 0	10 ± 0	10 ± 0	10 ± 0	10 ± 0	10 ± 0	10 ± 0
CK (68–1070 U/L)	645.7 ± 133.5	483.8 ± 85.7	736.3 ± 134.5	751.8 ± 247.6	581.0 ± 140.6	587.0 ± 36.9	466.0 ± 145.2	419.0 ± 49.4	974.0 ± 531.4	529.3 ± 220.2
OCN (ng/mL)	123.9 ± 15.4	NA	112.3 ± 6.8	139.9 ± 6.9	135.2 ± 18.9	139.7 ± 21.9	NA	142.6 ± 8.7	110.0 ± 9.3	120.4 ± 17.9
CTX (ng/mL)	20.7 ± 1.7	NA	18.7 ± 1.4	21.5 ± 1.3	13.8 ± 1.3	20.5 ± 1.6	NA	21.7 ± 1.7	17.7 ± 1.2	10.6 ± 0.9

Parameters are followed by mice normal range values and/or units in parentheses. Data are mean ± SEM, $n = 6$ mice/group except for OCN and CTX where $n = 5$ mice/group.

AGR = albumin-to-globulin ratio; BUN: blood urea nitrogen; Tot. bil.: total bilirubin; ALT: alanine transaminase; AST: aspartate transaminase; GGT: gamma-glutamyl transferase; LacCer = lactosylceramide; CK: creatine kinase; OCN: osteocalcin; CTX, carboxy-terminal collagen crosslinks; NA, not available; SEM = standard error of the mean.

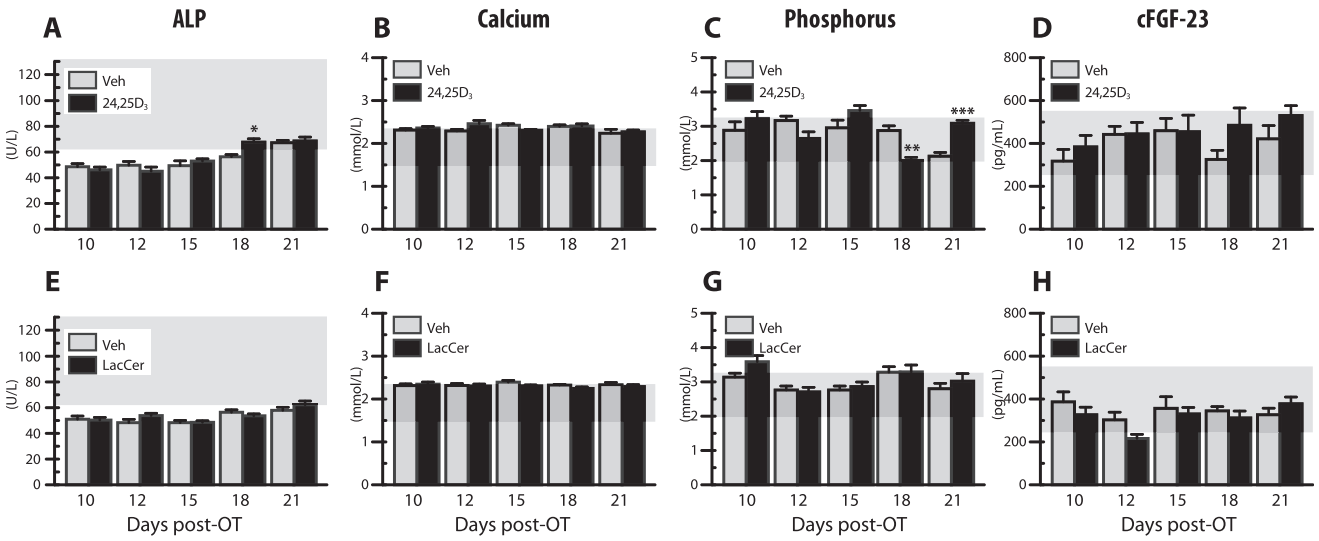

Figure 1. Effect of $24,25(OH)_2D_3$ or LacCer supplementation on mineral homeostasis during bone fracture repair in C57BL/6 mice. Twelve-week-old female mice were subcutaneously injected with $24,25(OH)_2D_3$ (6,7 μg/kg; A-D), LacCer (50 μg/kg; E-H) or propylene glycol vehicle (50 μL) from 3 to 21 days after osteotomy. The impact of either treatment on total serum ALP (A and E), calcaemia (B and F), phosphataemia (C and G) and c-terminal FGF23 (D and H) was monitored on Days 10, 12, 15, 18 and 21 post-OT. Shaded areas represent normal range for each parameter; not shown on graph, normal range for ALP extends to 209 U/L. $^*p < 0.05$; $^{**}p < 0.01$; $^{***}p < 0.001$ versus vehicle of corresponding time point; two-way analysis of variance (ANOVA) followed by Bonferroni post-test; $n = 7$ (ALP, Ca and P) or 8 (cFGF23). Data are mean ± standard error of the mean (SEM). $24,25D_3 = 24,25(OH)_2D_3$; ALP = alkaline phosphatase; LacCer = lactosylceramide; OT = osteotomy; Veh = vehicle.

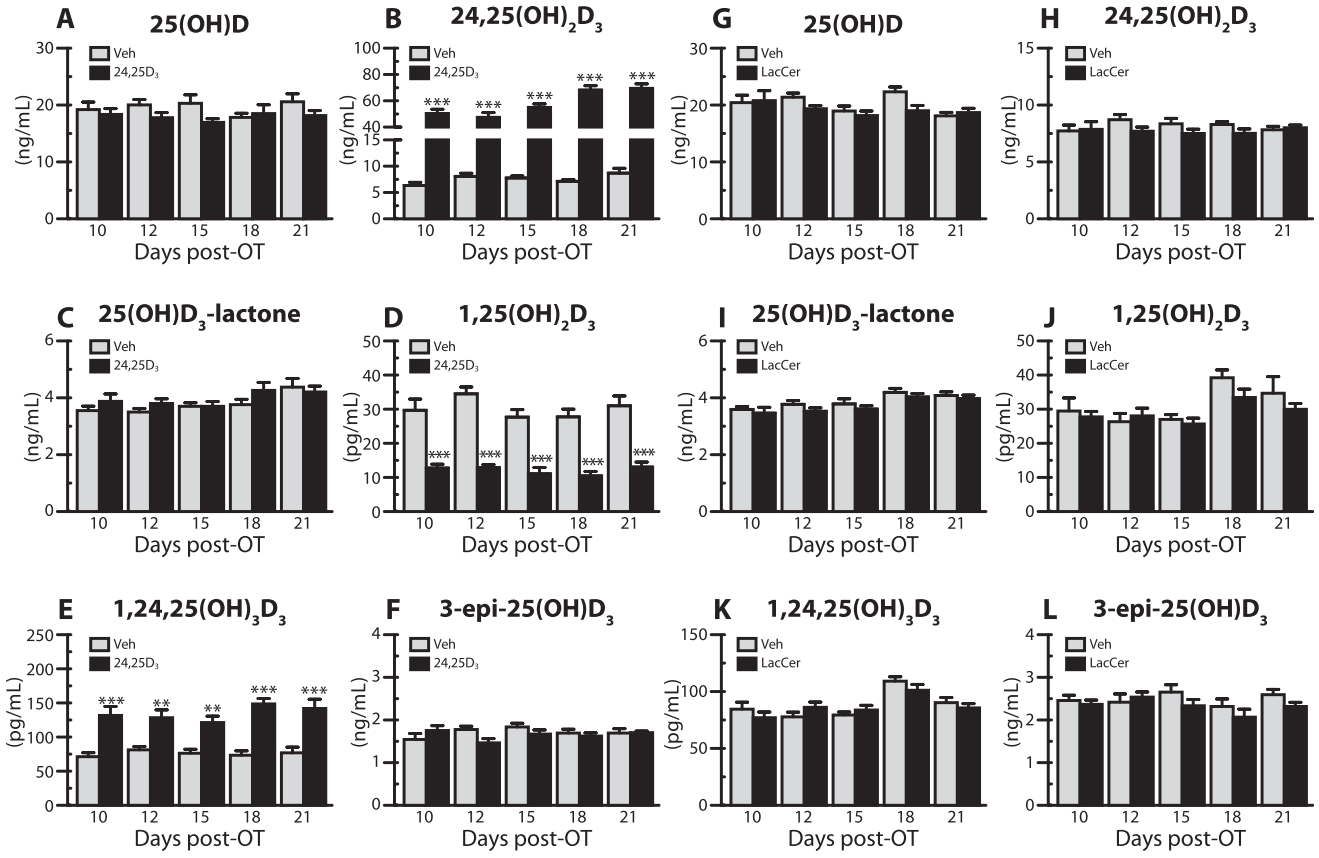

Figure 2. Effect of $24,25(OH)_2D_3$ or LacCer supplementation on circulating vitamin D metabolite levels during bone fracture repair in C57BL/6 mice. Twelve-week-old female mice were subcutaneously injected with $24,25(OH)_2D_3$ (6,7 μg/kg; A–F), LacCer (50 μg/kg; G–L) or propylene glycol vehicle (50 μL) from 3 to 21 days after osteotomy. Serum vitamin D metabolite levels were measured by liquid chromatography–tandem mass spectrometry (LC-MS/MS) after 4-[2-(3,4-Dihydro-6,7-dimethoxy-4-methyl-3-oxo-2-quinoxalinyl)ethyl]-3H-1,2,4-triazole-3,5(4H)-dione (DMEQ-TAD) derivatization. The metabolites $25(OH)D_3$ (A and G); $24,25(OH)_2D_3$ (B and H); $25(OH)D_3$-26,23-lactone ($25(OH)D_3$-lactone; C and I); $1,25(OH)_2D_3$ (D and J); $1,24,25(OH)_3D_3$ (E and K) and 3-epi-$25(OH)D_3$ (F and L) were monitored on Days 10, 12, 15, 18 and 21 post-OT. $^{**}p < 0.01$; $^{***}p < 0.001$ versus vehicle of corresponding time point, two-way ANOVA followed by Bonferroni post-test; $n = 8$. Data are mean ± SEM. $24,25D_3 = 24,25(OH)_2D_3$; LacCer = lactosylceramide; OT = osteotomy; Veh = vehicle.

Because phosphorus levels were found to modestly vary during the fracture repair process, and somewhat after $24,25(OH)_2D_3$ supplementation, c-terminal FGF23 (cFGF23) levels were assessed as it has been reported to be a marker of bone repair [17]. Serum levels of cFGF23 remained within normal ranges and neither time nor treatment was found to exert a significant effect on this parameter (Fig. 1D and H). Along with unchanged calcium levels, these cFGF23 levels are indicative of normal parathyroid hormone (PTH) response and mineral homeostasis [18].

Circulating vitamin D metabolites

No difference was detected in levels of $25(OH)D_3$ (Fig. 2A and G), $25(OH)D_3$-26,23-lactone (Fig. 2C and I) nor 3-epi-$25(OH)D_3$ (Fig. 2F and L) between either treatment or vehicle. As expected, subcutaneous injections of $24,25(OH)_2D_3$ increased circulating levels of this metabolite about eight-fold throughout the treatment (Fig. 2B), but LacCer injections had no measurable impact on circulating levels of this metabolite (Fig. 2H). A significant decrease was observed for $1,25(OH)_2D_3$ levels in $24,25(OH)_2D_3$-injected mice (Fig. 2D), but not in LacCer-treated animals (Fig. 2J). Levels of $1,24,25(OH)_3D_3$ were significantly increased in $24,25(OH)_2D_3$-treated mice (Fig. 2E), suggesting 1α-hydroxylation of $24,25(OH)_2D_3$ because the values exceeded that of $1,25(OH)_2D_3$ levels alone. We previously showed that $1,24,25(OH)_3D_3$ was produced in $24,25(OH)_2D_3$-dosed *Cyp24a1*$^{-/-}$ mice, confirming that $1,24,25(OH)_3D_3$ can be produced directly from a $24,25(OH)_2D_3$ dose via 1α-hydroxylation [13]. We also detected the presence of 24-oxo-$25(OH)D_3$, 24-oxo-$23,25(OH)_2D_3$ and calcioic acid in 24, $25(OH)_2D_3$-dosed animals at all time points postosteotomy (data not shown), revealing that $24,25(OH)_2D_3$ is likely cleared from the animal in a parallel manner as previously described for $1,25(OH)_2D_3$.

We observed relatively small variations in postfracture, time-dependent changes in ratios of circulating vitamin D metabolites, independently of treatment (Fig. 3). A significant decrease with time was measured for the $25(OH)D_3$:$24,25(OH)_2D_3$ ratio (Fig. 3A and D) as well as for the $25(OH)D_3$:$25(OH)D_3$-26,23-lactone ratio (Fig. 3B and E). The $1,25(OH)_2D_3$:$25(OH)D_3$ ratio—an index of hydroxylation efficiency [19]—was increased in the LacCer-treated cohort only.

When plotting the different metabolite levels against the $25(OH)D_3$ metabolite concentrations from which they are derived (Fig. 3G–I), $24,25(OH)_2D_3$ levels were found to positively correlate with $25(OH)_2D_3$ in vehicle- and LacCer-treated groups (r_S for vehicle = 0.7523, $p < 0.0001$; LacCer = 0.6817, $p < 0.0001$, respectively), but not in $24,25(OH)_2D_3$-treated groups ($r_S = 0.1997$, ns), indicative of a decoupling between these variables (Fig. 3G). A positive correlation between $25(OH)D_3$-26,23-lactone and $25(OH)D_3$ levels was observed in all three groups, but appeared weaker in LacCer-treated mice yet was stronger after $24,25(OH)_2D_3$ treatment (Fig. 3H, r_S for vehicle = 0.5255, $p < 0.0001$; 24,25D = 0.6909, $p < 0.0001$; LacCer = 0.3413, $p = 0.0311$). The $24,25(OH)_2D_3$ treatment

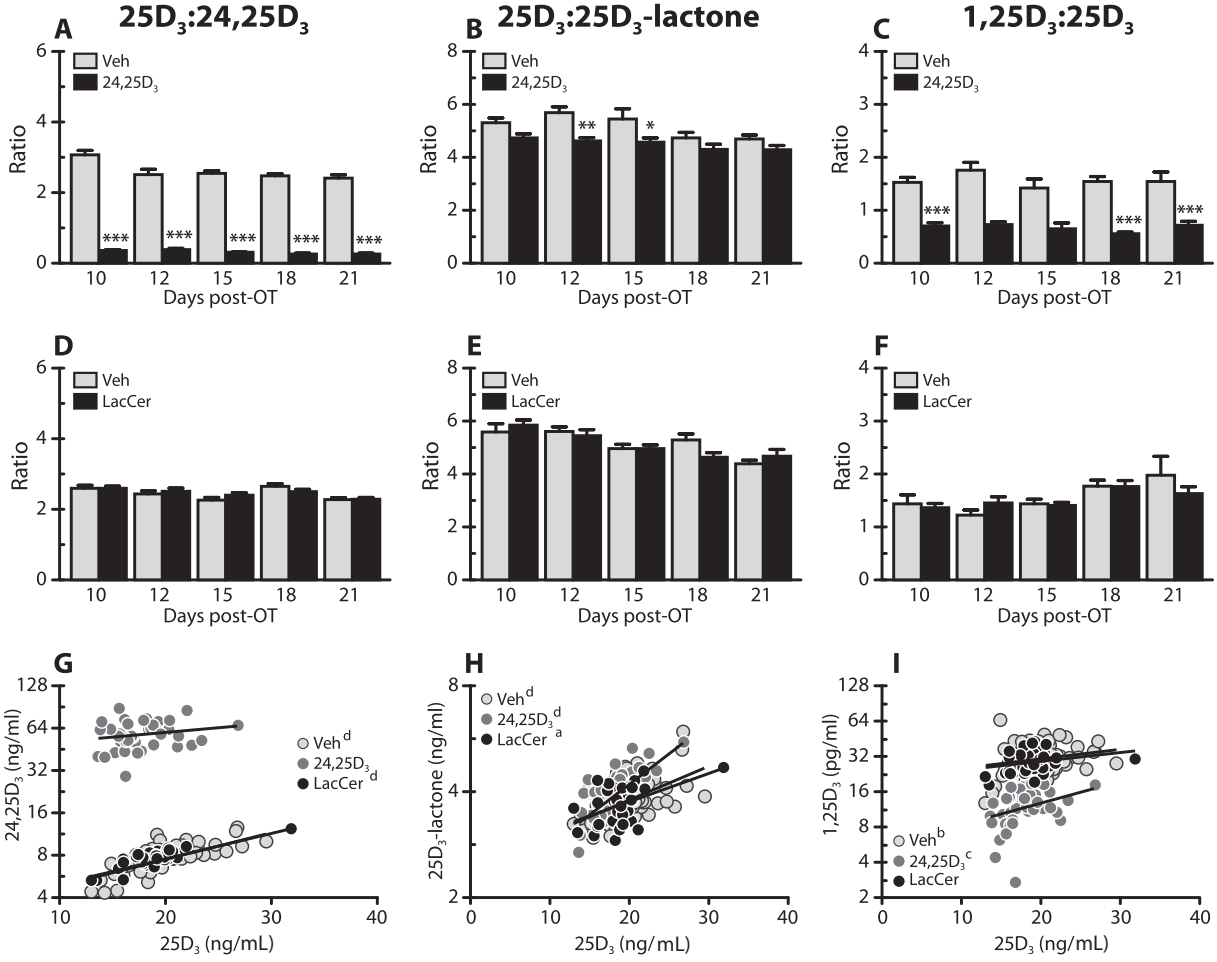

Figure 3. Effect of $24,25(OH)_2D_3$ or LacCer supplementation on circulating vitamin D metabolite ratios and hydroxylation efficiency during bone fracture repair in C57BL/6 mice. Data from Fig. 2 were used to visualize ratios between $25(OH)D_3$ and $24,25(OH)_2D_3$ ($25D_3$:$24,25D_3$; A and D), $25(OH)D_3$ and $25(OH)D_3$-26,23-lactone ($25D_3$:$25D_3$-lactone; B and E) and $1,25(OH)_2D_3$ and $25(OH)D_3$ ($1,25D_3$:$25D_3$; C and F) after $24,25(OH)_2D_3$ (A–C) or LacCer (D–F) treatment on Days 10, 12, 15, 18 and 21 post-OT. *$p < 0.05$; ** $p < 0.01$; ***$p < 0.001$ versus vehicle of corresponding time point, two-way ANOVA followed by Bonferroni post-test, $n = 8$. Data are mean ± SEM. G–I, impact of treatment on the strength of association between $25(OH)D_3$ and $24,25(OH)_2D_3$ (G), $25(OH)D_3$-26,23-lactone (H), or $1,25(OH)_2D_3$ (I) was evaluated using a nonparametric correlation analysis. [a]$p = 0.0311$; [b]$p = 0.0246$; [c]$p = 0.0024$; [d]$p < 0.0001$, nonparametric Spearman correlation, $n = 40$ per group. Each circle represents one data point. $24,25D_3 = 24,25(OH)_2D_3$; LacCer = lactosylceramide; OT = osteotomy; Veh = vehicle.

Table 3
Callus morphometric parameters in 12-week-old vehicle- or 24,25$(OH)_2D_3$-treated female C57BL/6 mice 10–21 days postosteotomy.

Treatment	Vehicle					24,25$(OH)_2D_3$				
Day	10 (9)	12 (8)	15 (8)	18 (8)	21 (8)	10 (9)	12 (8)	15 (6)	18 (9)	21 (9)
TV (mm^3)	8.61 ± 0.66	11.08 ± 0.94	14.82 ± 0.95	11.64 ± 1.01	9.98 ± 1.48	7.93 ± 0.34	10.21 ± 1.05	17.80 ± 0.94	11.12 ± 1.29	8.66 ± 0.94
BV (mm^3)	1.57 ± 0.14	2.22 ± 0.14	2.94 ± 0.16	2.62 ± 0.20	1.56 ± 0.23	1.39 ± 0.09	1.98 ± 0.22	**3.79 ± 0.22**[a]	2.42 ± 0.31	1.48 ± 0.16
BV/TV (%)	18.2 ± 0.4	20.4 ± 0.7	19.9 ± 0.3	22.7 ± 0.4	15.7 ± 0.6	17.4 ± 0.4	19.3 ± 0.8	21.4 ± 1.0	21.1 ± 1.1	17.0 ± 0.5
TS (mm^2)	100.8 ± 4.1	109.0 ± 5.0	120.6 ± 3.3	117.7 ± 4.2	98.7 ± 4.5	101.5 ± 2.4	106.1 ± 4.9	123.9 ± 2.4	110.8 ± 6.6	98.1 ± 3.7
BS (mm^2)	250.6 ± 23.2	336.7 ± 24.6	460.0 ± 32.3	366.9 ± 25.9	209.9 ± 30.5	230.7 ± 15.0	310.0 ± 39.2	**624.0 ± 38.2**[b]	332.6 ± 43.6	198.4 ± 21.3
iS (mm^2)	10.8 ± 0.6	15.8 ± 0.5	21.4 ± 0.3	23.2 ± 1.0	19.2 ± 0.9	10.6 ± 0.6	14.1 ± 0.9	21.0 ± 0.6	22.5 ± 1.6	19.0 ± 1.3
TbPf (mm^{-1})	43.4 ± 1.1	38.8 ± 1.0	42.8 ± 1.0	37.1 ± 0.6	39.4 ± 0.8	46.8 ± 1.0	40.7 ± 1.6	45.1 ± 2.1	38.5 ± 1.5	38.3 ± 0.8
SMI (unitless)	1.63 ± 0.03	1.54 ± 0.02	1.65 ± 0.02	1.59 ± 0.03	1.75 ± 0.03	1.69 ± 0.02	1.57 ± 0.03	1.64 ± 0.06	1.68 ± 0.06	1.71 ± 0.03
Conn (unitless)	41391.3 ± 4408.3	55182.3 ± 4815.7	74944.9 ± 7681.2	50260.5 ± 3808.6	20015.8 ± 3361.3	39261.5 ± 3332.7	52601.5 ± 7869.6	**119405.7 ± 13072.5**[c]	41478.5 ± 6550.7	20318.2 ± 3407.8
ConnDen (μm^{-1})	0.59 ± 0.02	0.62 ± 0.02	0.62 ± 0.03	0.55 ± 0.03	0.25 ± 0.02	0.61 ± 0.03	0.63 ± 0.04	**0.84 ± 0.08**[c]	0.44 ± 0.04	0.29 ± 0.04
pMMI (mm^4)	3.33 ± 0.38	4.51 ± 0.45	6.47 ± 0.57	4.86 ± 0.57	2.78 ± 0.56	2.99 ± 0.22	4.37 ± 0.73	**8.92 ± 0.76**[a]	4.50 ± 0.71	2.56 ± 0.39
FD (unitless)	2.43 ± 0.02	2.51 ± 0.01	2.59 ± 0.01	2.56 ± 0.01	2.46 ± 0.03	2.40 ± 0.02	2.47 ± 0.02	2.64 ± 0.01	2.53 ± 0.04	2.44 ± 0.02
vBMD (mg/mm^3)	1477 ± 0.008	1482 ± 0.008	1470 ± 0.011	1500 ± 0.006	1597 ± 0.011	1498 ± 0.011	1476 ± 0.018	**1410 ± 0.014**[a]	1509 ± 0.010	1585 ± 0.010

Each parameter is followed by units in parentheses; number of mice per group indicated in parentheses at top of each column. Significant differences observed on Day 15 in treated groups versus vehicle for BV, BS, Conn, ConnDen, pMMI and vBMD. Bold signifies statistically significant change vs. vehicle.
two-way ANOVA followed by Bonferroni post-test.
ANOVA = analysis of variance; BS = bone surface; BV = bone volume; BV/TV = mineralized tissue fraction; Conn = connectivity; ConnDen = connectivity density; FD = fractal dimension; iS = intersection surface; pMMI = mean polar moment of inertia; SMI = structure model index; TbPf = trabecular pattern factor; TS = tissue surface; TV = tissue volume; vBMD = volumetric bone mineral density.
[a] $p < 0.05$
[b] $p < 0.01$
[c] $p < 0.001$

Table 4
Morphometric callus parameters in 12-week-old vehicle- or LacCer-treated female C57BL/6 mice 10–21 days postosteotomy.

Treatment	Vehicle					LacCer				
Day	10 (7)	12 (7)	15 (7)	18 (7)	21 (7)	10 (6)	12 (7)	15 (7)	18 (7)	21 (7)
TV (mm^3)	9.11 ± 0.23	11.19 ± 0.98	11.41 ± 1.11	9.37 ± 0.52	9.38 ± 0.75	8.37 ± 0.71	11.11 ± 0.81	11.14 ± 1.39	7.65 ± 0.67	8.65 ± 0.91
BV (mm^3)	2.31 ± 0.08	3.14 ± 0.29	3.08 ± 0.31	2.23 ± 0.16	1.90 ± 0.16	1.95 ± 0.24	3.03 ± 0.23	3.08 ± 0.36	1.82 ± 0.17	1.84 ± 0.19
BV/TV (%)	25.3 ± 0.4	28.0 ± 0.3	27.0 ± 0.3	23.8 ± 0.6	20.4 ± 0.8	23.0 ± 1.1	27.2 ± 0.3	27.8 ± 0.5	23.7 ± 0.7	21.2 ± 0.5
TS (mm^2)	98.4 ± 1.8	102.6 ± 6.4	105.9 ± 5.3	95.2 ± 4.7	90.9 ± 3.3	91.3 ± 5.1	101.9 ± 2.6	102.1 ± 6.7	84.5 ± 3.6	85.9 ± 3.8
BS (mm^2)	292.3 ± 9.3	383.8 ± 37.7	371.9 ± 38.8	252.6 ± 19.9	206.9 ± 17.5	247.1 ± 29.9	377.1 ± 29.2	369.5 ± 48.0	202.0 ± 20.0	200.4 ± 20.4
iS (mm^2)	11.6 ± 0.2	16.7 ± 0.8	22.4 ± 1.0	20.9 ± 1.1	20.3 ± 0.8	11.3 ± 0.9	16.1 ± 0.9	22.0 ± 1.1	19.3 ± 1.0	19.2 ± 0.7
TbPf (mm^{-1})	27.2 ± 0.6	23.7 ± 0.9	27.8 ± 0.7	29.9 ± 0.7	30.5 ± 0.7	28.8 ± 0.8	25.5 ± 0.8	25.9 ± 0.8	29.5 ± 0.7	30.3 ± 0.6
SMI (unitless)	1.29 ± 0.02	1.17 ± 0.04	1.39 ± 0.03	1.59 ± 0.04	1.68 ± 0.04	1.36 ± 0.03	1.23 ± 0.03	1.30 ± 0.04	1.60 ± 0.03	1.66 ± 0.03
Conn (unitless)	44681.1 ± 1512.1	58904.4 ± 6834.4	46689.0 ± 6146.6	22976.4 ± 2353.6	16062.7 ± 1662.8	35900.8 ± 5217.2	58732.4 ± 5054.2	48865.0 ± 9045.9	17408.6 ± 2083.6	15965.3 ± 1987.4
ConnDen (μm^{-1})	1.06 ± 0.02	1.12 ± 0.05	0.87 ± 0.04	0.53 ± 0.04	0.37 ± 0.03	0.91 ± 0.07	1.14 ± 0.03	0.92 ± 0.06	0.48 ± 0.02	0.39 ± 0.02
pMMI (mm^4)	5.19 ± 0.28	6.66 ± 0.93	6.00 ± 0.83	3.83 ± 0.42	3.15 ± 0.36	4.08 ± 0.64	6.23 ± 0.63	5.86 ± 1.08	2.77 ± 0.35	2.91 ± 0.43
FD (unitless)	2.44 ± 0.01	2.51 ± 0.02	2.53 ± 0.02	2.48 ± 0.01	2.44 ± 0.01	2.41 ± 0.02	2.51 ± 0.02	2.54 ± 0.02	2.44 ± 0.02	2.43 ± 0.02
vBMD (mg/mm^3)	1358 ± 0.007	1386 ± 0.017	1411 ± 0.014	1477 ± 0.006	1533 ± 0.007	**1450 ± 0.029**[a]	1357 ± 0.011	1404 ± 0.014	1490 ± 0.008	1.558 ± 0.012

Each parameter is followed by units in parentheses; number of mice per group indicated in parentheses at top of each column. Statistically significant differences were observed on Day 10 in treated group versus vehicle for vBMD;
two-way ANOVA followed by Bonferroni post-test. Bold signifies statistically significant change vs. vehicle.
ANOVA = analysis of variance; BS = bone surface; BV = bone volume; BV/TV = mineralized tissue fraction; Conn = connectivity; ConnDen = connectivity density; FD = fractal dimension; iS = intersection surface; pMMI = mean polar moment of inertia; SMI = structure model index; TbPf = trabecular pattern factor; TS = tissue surface; TV = tissue volume; vBMD = volumetric bone mineral density.
[a] $p < 0.001$

somewhat strengthened the weak positive correlation between $1,25(OH)_2D_3$ and $25(OH)D_3$ levels, whereas LacCer treatment disrupted it altogether (Fig. 3I, r_S for vehicle = 0.2511, $p = 0.0246$; $24,25D_3 = 0.4675$, $p = 0.0024$; LacCer = 0.2788, ns).

Callus structure and mechanical properties

During fracture repair, the callus tissue volume and bone volume peaked around Day 15 postosteotomy (Tables 3 and 4), a time point corresponding to mineralization of the cartilaginous scaffold and the beginning of callus remodelling [5]. The $24,25(OH)_2D_3$ treatment (Table 3) significantly increased callus bone volume, bone surface, connectivity and connectivity density as well as mean polar moment of inertia versus vehicle-treated mice. vBMD was slightly reduced in Day 15 treated calluses (Table 3). LacCer treatment showed no measurable impact on callus size or structure (Table 4), but vBMD was increased by the treatment early in the sequence (Day 10; Table 4).

As illustrated in Fig. 4, both compounds showed greatest impact in bone mechanical properties on Day 18 postosteotomy. Again, this time point corresponds to peak endochondral mineralization and the beginning of the remodelling phases of healing. The effects of $24,25(OH)_2D_3$ and LacCer were mainly evident in parameters such as stiffness (Fig. 4A and G) and elastic modulus (Fig. 4B and H). Interestingly, each compound had slightly different effects on some mechanical parameters: $24,25(OH)_2D_3$ also significantly increased stiffness (Fig. 4A) and elastic modulus (Fig. 4B) on Day 10, whereas LacCer significantly enhanced load at yield (Fig. 4K) and strength at yield (Fig. 4L) on Day 18.

Expression of TLCD3B during fracture repair

Because the TLCD3B2 protein, the TLCD3B isoform most expressed in chondrocytes, has been demonstrated to be the effector protein binding $24,25(OH)_2D_3$ and subsequently producing LacCer [12], a TLCD3B global isoform antibody was used on undecalcified callus sections for each time point harvested (Fig. 5). TLCD3B2 was found to be expressed on Days 10 and 12 postosteotomy and to progressively recede to become undetectable by Day 18. TLCD3B2's presence in fracture callus seemed limited to the surface of unmineralized or pre-mineralized cartilage, respectively, visible as pink or purplish areas on the trichrome-stained sections (row A). By Day 18 postosteotomy, all that remained was nonspecific matrix binding of the secondary antibody.

Because TLCD3B2 was most highly expressed on Days 10 and 12 postosteotomy, the effect of the $24,25(OH)_2D_3$ or LacCer treatments on its expression was imaged (Fig. 6) and quantified (Fig. 7) at these time points. Both compounds at both time points reduced the number of TLCD3B2-positive cells (Fig. 7A and B). Again, as the cartilage mineralized (as illustrated by the blue areas in the trichrome-stained sections, Columns 1 and 4), the TLCD3B2 protein was restricted to the unmineralized or lightly mineralized areas of the callus (pinkish to purplish areas). The ratio of mineralized to unmineralized callus was significantly higher on Day 10 in $24,25(OH)_2D_3$-treated calluses as well as on Days 10 and 12 in LacCer-treated calluses (Fig. 7C and D). Fully mineralized

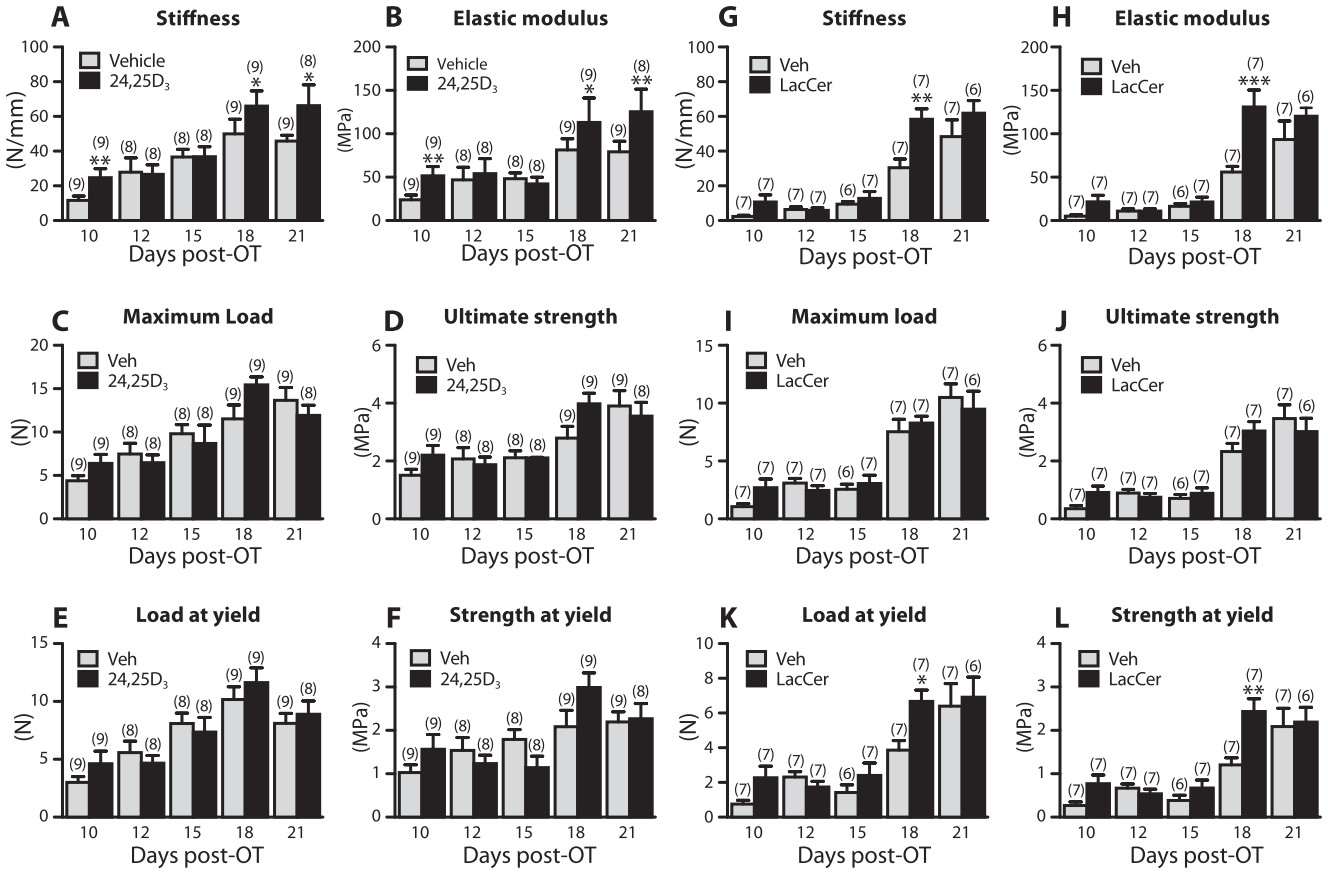

Figure 4. Mechanical properties of calluses from C57BL/6 mice supplemented with $24,25(OH)_2D_3$ or LacCer. Twelve-week-old female mice were subcutaneously injected with $24,25(OH)_2D_3$ (6,7 μg/kg; A–F), LacCer (50 μg/kg; G–L) or propylene glycol vehicle (50 μL) from 3 to 21 days post-OT. Parameters measured were bone stiffness (A and G), elastic modulus (B and H), maximum load (C and I), ultimate strength (D and J), load at yield (E and K) and strength at yield (F and L). $^*p < 0.05$; $^{**}p < 0.01$; $^{***}p < 0.001$ versus vehicle of corresponding time point; two-way ANOVA followed by Bonferroni post-test; number of mice per group indicated in parentheses above respective bar. Data are mean ± SEM. $24,25D_3 = 24,25(OH)_2D_3$; LacCer = lactosylceramide; OT = osteotomy; Veh = vehicle.

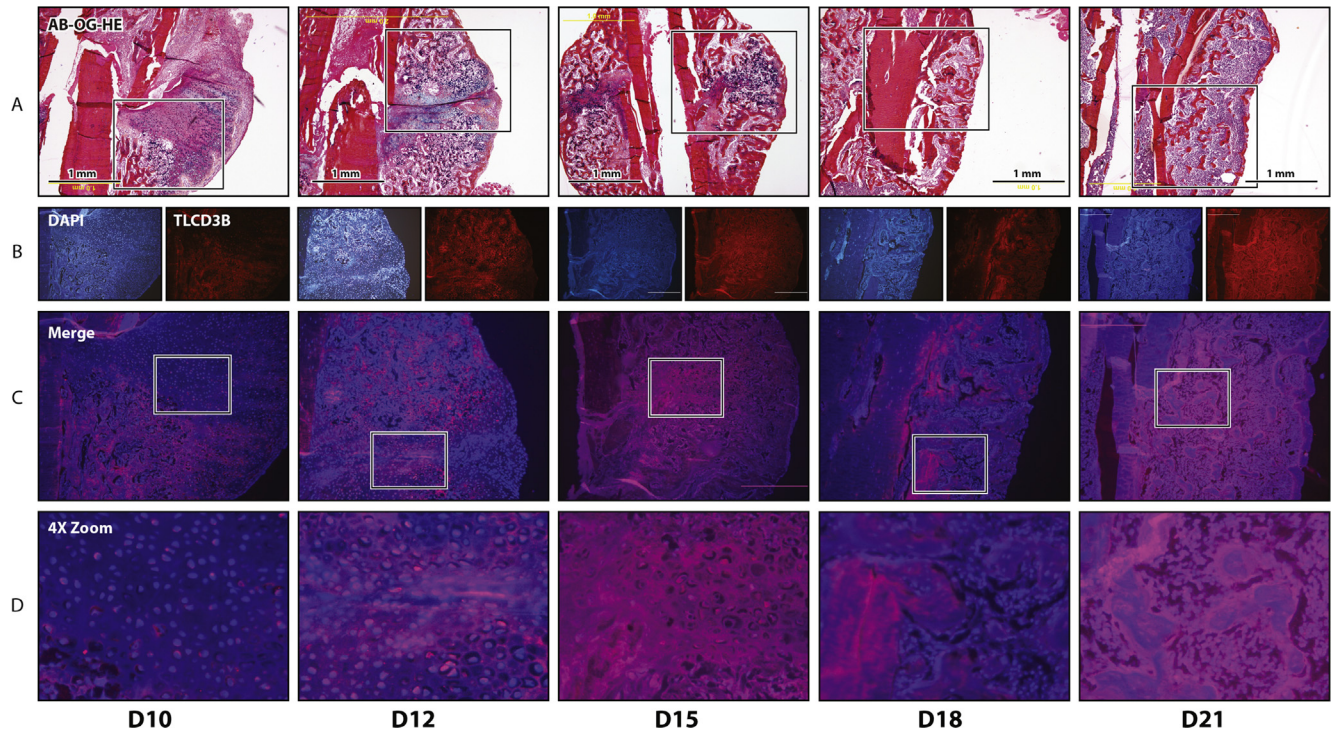

Figure 5. Expression of TLCD3B in callus tissue during fracture repair in C57BL/6 mice. Top row: AB-OG-HE trichrome staining of undecalcified methylmethacrylate-embedded callus tissues harvested at Days (D) 10, 12, 15, 18 and 21 postosteotomy. Squares represent areas for fluorescent imaging and 4× zoom in rows B–D. Scale bar = 1 mm. Representative images from three samples per group. AB-OG-HE = Alcian Blue-Orange G-Hematoxylin.

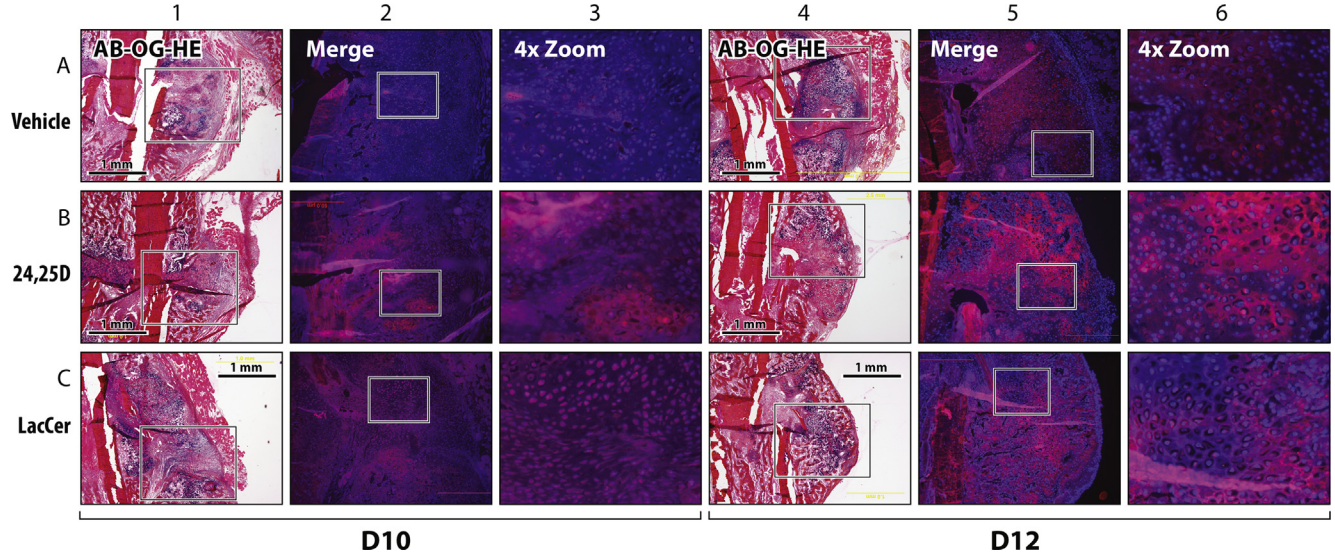

Figure 6. Effect of 24,25(OH)$_2$D$_3$ or LacCer supplementation on TLCD3B expression in Days 10 and 12 callus tissue of C57BL/6 mice. Columns 1 and 4: AB-OG-HE trichrome staining of undecalcified methylmethacrylate-embedded callus tissues harvested on Day 10 (D10, Columns 1–3) and Day 12 postosteotomy (D12, Columns 4–6) of vehicle- (row A), 24,25(OH)$_2$D$_3$- (row B) or LacCer- (row C) treated 12-week-old female mice. Scale bar = 1 mm. Columns 2 and 5: merged images of anti-TLCD3B (red) and DAPI (blue) of selected areas in Columns 1 and 4, respectively. Columns 3 and 6: 4× digital zoom of white square selected in images from Columns 2 and 5, respectively. Representative images from two (LacCer, D10) to three samples per group. AB-OG-HE = Alcian Blue-Orange G-Hematoxylin; LacCer = lactosylceramide.

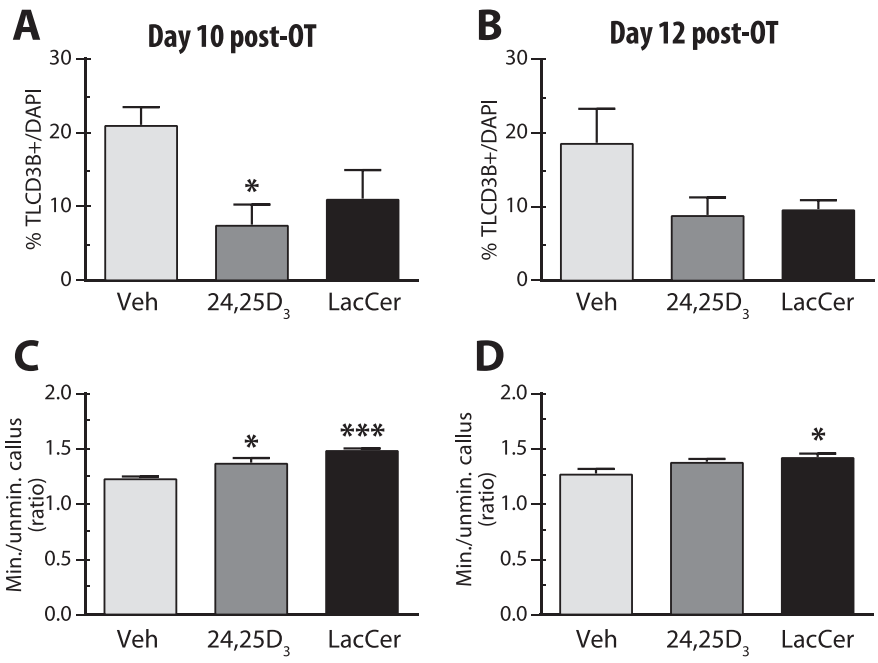

Figure 7. Quantification of TLCD3B-positive cells and mineralized versus unmineralized area in Days 10 and 12 callus tissue from inbred mice supplemented with 24,25(OH)$_2$D$_3$ or LacCer. Ratio of TLCD3B-positive cells per DAPI-stained in Day 10 (A) and Day 12 (B) postfracture callus tissue sections. Cells were counted with ImageJ within four regions of interest of 200 × 265 μm per image, for at least two images per sample, then averaged. *$p < 0.05$; **$p < 0.01$; ***$p < 0.001$, one-way ANOVA followed by Dunnett's post-test. Ratio of mineralized versus unmineralized cartilage in Day 10 (C) and Day 12 (D) callus tissue sections. Mineralized versus unmineralized callus tissue areas were measured with ImageJ within two regions of interest per sample comprising each half the callus, then averaged and expressed as a ratio. Three (Day 10) to four (Day 12) samples per group. 24,25D$_3$ = 24,25(OH)$_2$D$_3$; LacCer = lactosylceramide; Veh = vehicle.

cartilage and bone tissue (in bright pink/pinkish orange, Fig. 6) did not express TLCD3B2. TLCD3B2 was not detected in treated samples on Days 15, 18 nor 21 (data not shown).

Discussion

The vitamin D metabolite, 24,25(OH)$_2$D$_3$, and LacCer were found to rescue callus formation in *Cyp24a1*-null mice [12]. We aimed to assess their safety and efficacy in wild-type mice. A secondary objective was to determine which time range to consider for treatment.

Safety of 24,25(OH)$_2$D$_3$ or LacCer treatment in inbred, nongenetically modified mice

No toxicity of either 24,25(OH)$_2$D$_3$ or LacCer was observed, as ALT and AST levels were unaltered, and GGT levels remained below detectable threshold [20]. The sustained low albumin and creatinine levels measured in all groups were likely caused by increased metabolic clearance [21]. Because the same effect was observed in all groups, this might be linked to the propylene glycol vehicle, known to induce alcohol and lactate dehydrogenase and to increase urinary excretion in mammals [22]. Another factor is the increased demand on kidney function caused by bone repair itself [23]. Indeed, some studies suggest delayed fracture healing in experimental animals suffering kidney disease [24], underscoring the importance of optimal kidney function during bone repair.

Wound healing in general increases metabolic demand in ATP [15]. The present data supports this statement with higher serum levels of glucose—used by osteoblasts during aerobic glycolysis [25]—and total ALP—increasing the amount of free inorganic phosphate [26]. The latter may also reflect increased bone ALP during mineralization, agreeing with higher phosphorus levels necessary for hydroxyapatite formation [27]. This observation is reinforced by the time point of increased ALP, specifically on Days 18 and 21. Although high ALP levels early on might reflect liver damage [20], an absence of ALP increase would suggest no callus formation symptomatic of a nonunion [28]. Although cFGF23 was reported to be a marker of bone fracture repair [17], our data suggest that this hormone is not involved in mediating the effects of 24,25(OH)$_2$D$_3$ and LacCer.

Effect of fracture healing and treatment on vitamin D metabolism

As expected, subcutaneous injections of 24,25(OH)$_2$D$_3$ significantly increased circulating levels of 24,25(OH)$_2$D$_3$ and 1,24,25(OH)$_3$D$_3$. Interestingly, this treatment also significantly reduced levels of 1,25(OH)$_2$D$_3$. Taken together, these data suggest that CYP27B1 used 24,25(OH)$_2$D$_3$ as a substrate for 1,24,25(OH)$_3$D$_3$ production instead of converting 25(OH)D$_3$ into 1,25(OH)$_2$D$_3$. Indeed, competitive inhibition of 25(OH)D$_3$ 1α-hydroxylation by high 24,25(OH)$_2$D$_3$ levels has been reported in calcium-deficient rats [29], as well as in *Cyp24a1*-deficient mice [13]. The LacCer-treated group showed no measurable difference in any of the vitamin D metabolites, suggesting little interaction with vitamin D metabolizing enzymes. The present data demonstrated that 24,25(OH)$_2$D$_3$ treatment had the most impact on vitamin D metabolism, illustrated by the loss of positive correlation between 25(OH)D$_3$ and 24,25(OH)$_2$D$_3$ in the 24,25(OH)$_2$D$_3$-treated mice, where the rate of conversion is independent of the 25(OH)D$_3$ metabolite from which it is derived. Treatment with 24,25(OH)$_2$D$_3$ probably also modulated CYP27B1 substrate selectivity, but this had no major impact on mineral ion homeostasis.

On the other hand, it was found that the fracture healing process systematically increased circulating levels of 25(OH)D$_3$-26,23-lactone independently of treatment. This metabolite results from the C23-hydroxylation of 25(OH)D$_3$ by the CYP24A1 enzyme [30] and is largely thought to be inactive. However, some authors claim that the 26,23-lactone compounds of both 1,25(OH)$_2$D$_3$ and 25(OH)D$_3$ increase intestinal calcium absorption and reduce bone calcium mobilization in chicks [30]. Although these functions could be relevant in the context of fracture repair, no data exist in mammals as of yet. Moreover, our data indicate very stable serum calcium levels during the observed time range. Changes at later time points, beyond the endochondral ossification phase, cannot be excluded.

Efficacy of 24,25(OH)$_2$D$_3$ or LacCer in enhancing fracture repair in nongenetically modified mice

There is yet to be a consensus on the effect of vitamin D$_3$ on bone healing [8]. Indeed, beneficial effects of vitamin D$_3$ supplementation

during fracture repair mainly seems conclusive in cases of underlying deficiency or chronic kidney disease [24] in mice. Time of intervention might also be a factor, as 1,25-dihydroxyvitamin D_3 supplementation in normal mice during the inflammatory phase impairs bone healing by promoting M2 macrophage differentiation and inhibiting precursor cell migration at the wound site [31]. Interestingly, a decrease in serum levels of 1,25-dihydroxyvitamin D_3 postfracture has been reported in humans [11]. Whether these effects are solely dependent on direct vitamin D receptor (VDR) targets or also secondary to CYP24A1-induced 24-hydroxylation remains undetermined.

Bone resorption, as evaluated by measuring levels of the CTX biomarker, was unaffected by either treatment. The OCN bone formation marker was found to be significantly reduced on Day 18 of $24,25(OH)_2D_3$ treatment. This might be related to the fact that during fracture repair, OCN is mainly expressed in the unmineralized to mineralized transition zone of the callus, which disappears during the remodelling phase [32].

Both $24,25(OH)_2D_3$ and LacCer significantly ameliorated mechanical outcome of the callus during healing. Both compounds enhanced callus formation during the endochondral phase. We have reported that chondrogenic ATDC5 cells stably overexpressing *Tlcd3b2* showed elevated type 2 (*Col2a1*) and type 10 (*Col10a1*) collagen gene expression and increased proteoglycan synthesis [33]. Treatment of *Tlcd3b2*-overexpressing ATDC5 cells with $24,25(OH)_2D_3$ further increased the expression of *Col2a1*. Treatment of untransfected ATDC5 cells with LacCer enhanced chondrocyte maturation [33]. Overall, results from these studies strongly support a role for TLCD3B2 and LacCer in chondrocyte maturation and confirm the hypothesis that TLCD3B2 is involved in the endochondral stage of bone fracture healing by optimizing the maturation and potentially the hypertrophy of chondrocytes.

Moreover, recent work from van der Meijden et al. [34] demonstrated that primary human osteoblasts actively synthesize $24,25(OH)_2D_3$ *in vitro*, which increases ALP, OCN and osteopontin mRNA [34], suggesting a role in osteoblast biomineralization. Microvesicles are known to be the site of hydroxyapatite nucleation during biomineralization [35]. Microvesicles are shed from lipid rafts, plasma membrane microdomains enriched in cholesterol, sphingomyelin and LacCer [35]. Thus, perhaps $24,25(OH)_2D_3$ stimulates biomineralization during fracture repair by a dual mechanism: through the induction of matrix mineralizing protein expression and through the LacCer-producing activity of TLCD3B2.

We did not perform direct comparison of the effects of $24,25(OH)_2D_3$ and LacCer with known bone anabolic agents. Recombinant BMP-2 has been tested for the treatment of fresh, open tibial fractures but a double-blind, randomized controlled trial concluded that the times to fracture union were not substantially reduced by BMP-2 treatment [36]. Treatment with PTH has also been shown to be efficacious for fracture repair in postmenopausal women [37]. However, the FDA recommends against treatment with PTH (teriparatide) for children and adolescents whose bones are still growing. Thus, our preclinical results could be translated into a therapeutic modality for a juvenile population, such as patients with osteogenesis imperfecta [38].

Time range for most efficient treatment

Bone fracture repair essentially recapitulates embryonic bone formation [5]. The soft callus is a transient cartilage anlage, formed through mesenchymal condensation, undergoing hypertrophy, calcification and remodelling into lamellar bone, tightly regulated by numerous internal and external cues [6]. The callus being avascular, it remains debated how circulating compounds might reach the wound site. It has long been suspected that lipids play a significant role at this level as they facilitate passive diffusion before vascularization takes place [39] and participate to the formation of calcium hydroxyapatite crystals [40]. Indeed, matrix vesicles—enriched in cholesterol, phospholipids and glycolipids [35]—are the site of hydroxyapatite nucleation [26].

Although the strongest effect for both treatments manifested on Day 18, the present data demonstrate that expression of the TLCD3B2 effector protein is highest 10–12 days postosteotomy. Moreover, downregulation of the protein by either compound was most obvious at these time points, suggesting efficient targeting of the callus tissue before the onset of mineralization. The decrease in TLCD3B2 protein expression mimics the reduction in *Tlcd3b2* expression after treatment with $24,25(OH)_2D_3$ that we previously reported in the fracture callus and cultured chondrocytes [12]. The time lag between TLCD3B2 peak expression and maximal mechanical properties is probably due to the cell proliferation, differentiation and mineralization periods necessary for endochondral ossification [6]. Our data suggest that $24,25(OH)_2D_3$ or LacCer administration should occur before initiation of callus mineralization, during peak TLCD3B2 expression. This seems particularly relevant for $24,25(OH)_2D_3$ supplementation as stiffness and elastic modulus were both increased on Day 10 postosteotomy.

Conclusion

The present data demonstrate that both $24,25(OH)_2D_3$ and LacCer significantly increase mechanical properties of the callus in wild-type, nongenetically modified mice. Neither compound was found to exhibit any nephro- nor hepato-toxicity. However, the $24,25(OH)_2D_3$ treatment did show significant impact on vitamin D metabolism, namely higher levels of $24,25(OH)_2D_3$ and $1,24,25(OH)_3D_3$, as well as lower levels of $1,25(OH)_2D_3$. These effects are a direct consequence of the administration of the compound, which remains safe because calcaemia was not affected in the least. As $24,25(OH)_2D_3$ impacted both callus structure and mechanical properties, it seems to have a broader range of activity than LacCer, which only influenced mechanical properties.

Author contributions

All authors have read the journal's authorship statement. CM, MK and AA performed the experiments. CM, MK, AA, GJ, and RStA participated in data analysis and interpretation. RStA obtained the funding. CM and RStA participated in the conception and design of the study and wrote the manuscript. CM, MK, GJ and RStA read, corrected and approved the submitted manuscript.

Funding and role of funding sources

This work was supported by NIH grant R01 AR070544 (to RStA). CM is a postdoctoral fellow of the *Fonds de Recherche Québec – Santé*. The *Réseau de recherche en santé buccodentaire et osseuse* (RSBO) provided support to the bone phenotyping platform used in this study. The funding sources were not involved in study design nor in the collection, analysis and interpretation of data; in the writing of the report; or in the decision to submit the article for publication.

Conflict of Interest

Dr St-Arnaud is the named inventor on US Patents No. 13/905,985; 13/306,599; 13/906,014; 13/906,028: "A Cloned Transmembrane Receptor for 24-Hydroxylated Vitamin D Compounds and Uses Thereof" describing the cloning of the LacCer synthase FAM57B2 (Human Genome Organization Gene Nomenclature Committee approved gene name and symbol: TLC domain containing 3B isoform 2, TLCD3B2).

Acknowledgements

Through a Queen's University and Waters Corporation agreement, Waters provided the LC-MS/MS instrument used in this study. The authors thank Mark Lepik for final figures preparation, as well as Mia Esser and Louise Marineau (Shriners Hospitals for Children – Canada) for expert animal care.

References

[1] Zengin A, Prentice A, Ward KA. Ethnic differences in bone health. Front Endocrinol (Lausanne) 2015;6:24.
[2] Harvey NC, McCloskey EV, Mitchell PJ, Dawson-Hughes B, Pierroz DD, Reginster JY, et al. Mind the (treatment) gap: a global perspective on current and future strategies for prevention of fragility fractures. Osteoporos Int 2017;28(5):1507–29.
[3] Wekre LL, Eriksen EF, Falch JA. Bone mass, bone markers and prevalence of fractures in adults with osteogenesis imperfecta. Arch Osteoporos 2011;6:31–8.
[4] Borland S, Gaffey A. Congenital and metabolic disorders leading to fracture. Trauma 2012;14(3):243–56.
[5] Morgan EF, De Giacomo A, Gerstenfeld LC. Overview of skeletal repair (fracture healing and its assessment). Methods Mol Biol 2014;1130:13–31.
[6] Staines KA, Pollard AS, McGonnell IM, Farquharson C, Pitsillides AA. Cartilage to bone transitions in health and disease. J Endocrinol 2013;219(1):R1–12.
[7] Drissi H, Paglia DN, Alaee F, Yoshida R. Constructing the toolbox: patient-specific genetic factors of altered fracture healing. Genes Dis 2014;1(2):140–8.
[8] Gorter EA, Krijnen P, Schipper IB. Vitamin D status and adult fracture healing. J Clin Orthop Trauma 2017;8(1):34–7.
[9] Eschle D, Aeschlimann AG. Is supplementation of vitamin d beneficial for fracture healing? A short review of the literature. Geriatr Orthop Surg Rehabil 2011;2(3):90–3.
[10] Seo EG, Einhorn TA, Norman AW. 24R,25-dihydroxyvitamin D3: an essential vitamin D3 metabolite for both normal bone integrity and healing of tibial fracture in chicks. Endocrinology 1997;138(9):3864–72.
[11] Briggs AD, Kuan V, Greiller CL, Maclaughlin BD, Ramachandran M, Harris T, et al. Longitudinal study of vitamin D metabolites after long bone fracture. J Bone Miner Res 2013;28(6):1301–7.
[12] Martineau C, Naja RP, Husseini A, Hamade B, Kaufmann M, Akhouayri O, et al. Optimal bone fracture repair requires 24R,25-dihydroxyvitamin D3 and its effector molecule FAM57B2. J Clin Invest 2018;128(8):3546–57.
[13] Kaufmann M, Martineau C, Arabian A, Traynor M, St-Arnaud R, Jones G. Calcioic acid: in vivo detection and quantification of the terminal C24-oxidation product of 25-hydroxyvitamin D_3 and related intermediates in serum of mice treated with 24,25-dihydroxyvitamin D_3. J Steroid Biochem Mol Biol 2019;188:23–8.
[14] Erben RG. Embedding of bone samples in methylmethacrylate: an improved method suitable for bone histomorphometry, histochemistry, and immunohistochemistry. J Histochem Cytochem 1997;45(2):307–13.
[15] Demling RH. Nutrition, anabolism, and the wound healing process: an overview. Eplasty 2009;9:e9.
[16] Song SH, Lee H, Jeong JM, Cho WI, Kim SE, Song HR. The significance of serum phosphate level on healing index and its relative effects in skeletally immature and mature patients with hypophosphatemic rickets. BioMed Res Int 2014;2014:569530.
[17] Goebel S, Lienau J, Rammoser U, Seefried L, Wintgens KF, Seufert J, et al. FGF23 is a putative marker for bone healing and regeneration. J Orthop Res 2009;27(9):1141–6.
[18] Goltzman D, Mannstadt M, Marcocci C. Physiology of the calcium-parathyroid hormone-vitamin D Axis. Front Horm Res 2018;50:1–13.
[19] Pasquali M, Tartaglione L, Rotondi S, Muci ML, Mandanici G, Farcomeni A, et al. Calcitriol/calcifediol ratio: an indicator of vitamin D hydroxylation efficiency? BBA Clin 2015;3:251–6.
[20] Gowda S, Desai PB, Hull VV, Math AA, Vernekar SN, Kulkarni SS. A review on laboratory liver function tests. Pan Afr Med J 2009;3:17–28.
[21] Sasaki Y, Iwama R, Sato T, Heishima K, Shimamura S, Ichijo T, et al. Estimation of glomerular filtration rate in conscious mice using a simplified equation. Phys Rep 2014;2(8):e12135.
[22] ACo Toxicology. Final report on the safety assessment of propylene glygol and polypropylene glycols. Int J Toxicol 1994;13:437.
[23] Wei K, Yin Z, Xie Y. Roles of the kidney in the formation, remodeling and repair of bone. J Nephrol 2016;29(3):349–57.
[24] Liu W, Zhang S, Zhao D, Zou H, Sun N, Liang X, et al. Vitamin D supplementation enhances the fixation of titanium implants in chronic kidney disease mice. PloS One 2014;9(4):e95689.
[25] Esen E, Long F. Aerobic glycolysis in osteoblasts. Curr Osteoporos Rep 2014;12(4):433–8.
[26] Simao AM, Bolean M, Hoylaerts MF, Millan JL, Ciancaglini P. Effects of pH on the production of phosphate and pyrophosphate by matrix vesicles' biomimetics. Calcif Tissue Int 2013;93(3):222–32.
[27] Golub EE, Boesze-Battaglia K. The role of alkaline phosphatase in mineralization. Curr Opin Orthop 2007;18(5):444–8.
[28] Komnenou A, Karayannopoulou M, Polizopoulou ZS, Constantinidis TC, Dessiris A. Correlation of serum alkaline phosphatase activity with the healing process of long bone fractures in dogs. Vet Clin Pathol 2005;34(1):35–8.
[29] Matsumoto T, Ikeda K, Yamato H, Morita K, Ezawa I, Fukushima M, et al. Effect of 24,25-dihydroxyvitamin D3 on 1,25-dihydroxyvitamin D3 metabolism in calcium-deficient rats. Biochem J 1988;250(3):671–7.
[30] Prosser DE, Kaufmann M, O'Leary B, Byford V, Jones G. Single A326G mutation converts human CYP24A1 from 25-OH-D3-24-hydroxylase into -23-hydroxylase, generating 1alpha,25-(OH)2D3-26,23-lactone. Proc Natl Acad Sci USA 2007;104(31):12673–8.
[31] Wasnik S, Rundle CH, Baylink DJ, Yazdi MS, Carreon EE, Xu Y, et al. 1,25-Dihydroxyvitamin D suppresses M1 macrophages and promotes M2 differentiation at bone injury sites. JCI Insight 2018;3(17):e98773.
[32] Hu DP, Ferro F, Yang F, Taylor AJ, Chang W, Miclau T, et al. Cartilage to bone transformation during fracture healing is coordinated by the invading vasculature and induction of the core pluripotency genes. Development 2017;144(2):221–34.
[33] Antonyan L, Martineau C, St-Arnaud R. The ER protein TLC domain 3B2 and its enzymatic product lactosylceramide enhance chondrocyte maturation. Connect Tissue Res, in press; doi: 10.1080/03008207.2019.1657425.
[34] van der Meijden K, Lips P, van Driel M, Heijboer AC, Schulten EA, den Heijer M, et al. Primary human osteoblasts in response to 25-hydroxyvitamin D3, 1,25-dihydroxyvitamin D3 and 24R,25-dihydroxyvitamin D3. PloS One 2014;9(10):e110283.
[35] Bottini M, Mebarek S, Anderson KL, Strzelecka-Kiliszek A, Bozycki L, Simao AMS, et al. Matrix vesicles from chondrocytes and osteoblasts: their biogenesis, properties, functions and biomimetic models. Biochim Biophys Acta Gen Subj 2018;1862(3):532–46.
[36] Lyon T, Scheele W, Bhandari M, Koval KJ, Sanchez EG, Christensen J, et al. Efficacy and safety of recombinant human bone morphogenetic protein-2/calcium phosphate matrix for closed tibial diaphyseal fracture: a double-blind, randomized, controlled phase-II/III trial. J Bone Joint Surg Am 2013;95(23):2088–96.
[37] Aspenberg P, Genant HK, Johansson T, Nino AJ, See K, Krohn K, et al. Teriparatide for acceleration of fracture repair in humans: a prospective, randomized, double-blind study of 102 postmenopausal women with distal radial fractures. J Bone Miner Res 2010;25(2):404–14.
[38] Munns CF, Rauch F, Zeitlin L, Fassier F, Glorieux FH. Delayed osteotomy but not fracture healing in pediatric osteogenesis imperfecta patients receiving pamidronate. J Bone Miner Res 2004;19(11):1779–86.
[39] Villalvilla A, Gomez R, Largo R, Herrero-Beaumont G. Lipid transport and metabolism in healthy and osteoarthritic cartilage. Int J Mol Sci 2013;14(10):20793–808.
[40] Dean DD, Schwartz Z, Bonewald L, Muniz OE, Morales S, Gomez R, et al. Matrix vesicles produced by osteoblast-like cells in culture become significantly enriched in proteoglycan-degrading metalloproteinases after addition of beta-glycerophosphate and ascorbic acid. Calcif Tissue Int 1994;54(5):399–408.